

Effect of silver doping on the phase transformation and grain growth of sol-gel titania powder

H.E. Chao^{a,*}, Y.U. Yun^a, H.U. Xingfang^a, A. Larbot^b

^aResearch and Development Center for Special Inorganic Materials, Shanghai Institute of Ceramics, Chinese Academy of Sciences, Shanghai 200050, PR China

^bInstitut Européen de Membranes, (UMR 5635-CNRS, ENSCM, UM II), Campus CNRS, F-34293 Montpellier, France

Received 5 July 2002; received in revised form 10 September 2002; accepted 16 September 2002

Abstract

Pure and Ag doped TiO₂ powders were prepared by the sol-gel process. The effect of Ag doping on TiO₂ anatase to rutile phase transformation was investigated by means of XRD, TEM, SEM, DSC-TG, and surface morphological characterization. It is found that the Ag doping promotes the phase transformation but has a depression effect on the anatase grain growth. The mechanism is proposed. With a suitable amount (ca. 2–6 mol%), the Ag dopant reduces anatase grain size and increases the specific surface area of TiO₂ powder, which exhibits a great potential in improving the TiO₂ photocatalytic activity.

© 2002 Elsevier Science Ltd. All rights reserved.

Keywords: Ag; Grain growth; Phase transformation; Sol-gel processes; TiO₂

1. Introduction

During the past two decades, titania (TiO₂) has received great attentions due to its unique photocatalytic activity in the treatment of environmental contaminants. Numerous work have been carried out displaying its promising performance in degradating a wide variety of organic and inorganic pollutants such as DDT, dichloronitrobenzene, trichlorethylene, H₂S, NO, and Cr (VI), etc.^{1–3} But for practical application, the photocatalytic activity of TiO₂ needs further improvement. An effective way to improve the TiO₂ photoactivity is to introduce foreign metal ions into TiO₂. The sol-gel process is a most attractive method to introduce foreign metal ions into TiO₂ powders and films. Using this method, it is very easy to prepare homogenous ion-doped TiO₂ powders and films on various types of supports under mild conditions. Many works employed the method to introduce foreign metals ions, such as Cu²⁺,⁴

Fe³⁺,^{5,6} Pt⁴⁺,⁷ V⁵⁺,⁸ W⁶⁺ and Zn²⁺,⁶ etc., into TiO₂ powders and films. And the TiO₂ photocatalytic activity was improved to varying extents. The foreign metal ions, however, usually affect the TiO₂ phase transformation behavior and structure while they were introduced by sol-gel method. For example, by providing nuclei or increasing the concentration of anion vacancies formed by reduction of foreign ions in anatase grains, Cu²⁺, Fe³⁺, Pt⁴⁺ and V⁵⁺ promote both the TiO₂ anatase to rutile phase transformation and grain growth decreasing the thermal stability of sol-gel TiO₂.^{9–11} It is therefore interesting and necessary to examine the effect of foreign metal additives on the TiO₂ phase transformation and grain growth before their application.

In our previous work, using the sol-gel method we prepared Ag doped TiO₂ films and found that Ag could also effectively improve the photocatalytic activity of TiO₂ films.¹² However, no detailed study has been reported on the influence of Ag doping on the phase transformation and structure of sol-gel TiO₂. With a view to understanding those, using sol-gel process we prepared pure and Ag doped TiO₂ powders and investigated the effect of Ag doping on the TiO₂ anatase to rutile phase transformation and anatase grain growth.

* Corresponding author. Tel.: +86-21-5241-1021; fax: +86-21-5241-3903.

E-mail address: hechao@mail.sic.ac.cn (H.E. Chao).

2. Experimental procedure

2.1. Sample preparation

A 0.5 M TiO₂ sol was prepared by dropping proportional tetrabutyl orthotitanate and acetylacetone into ethyl alcohol at room temperature. After stirred for 30 min, certain amounts of water and nitric acid were added into the solution. The solution was successively stirred till a clear and transparent sol was obtained. The TiO₂ sol was dried at 100 °C in air for several days to get TiO₂ xerogel. Then the xerogel was calcined at different temperatures for 30 min to prepare TiO₂ powders. The Ag doped TiO₂ sol and powder were prepared by the same procedure as established above. The only difference was the addition of silver nitrate solution into the TiO₂ sol with nitric acid as stabilizer. The Ag concentration studied were 2, 4, 6, 8, 10 mol%, respectively.

For some property investigation pure and Ag doped TiO₂ films were prepared on Si and glass substrates by the dip-coating process. After being placed in air for several hours, the TiO₂ films were heat-treated at 500 °C for 30 min sequentially. The procedure was repeated several times to obtain a film with a certain thickness.

2.2. Analysis

X-ray diffraction (XRD) analysis of TiO₂ powders was carried out on a Siemens D5000V X-ray diffractometer, employing Cu-K_α(Ni filtered) radiation of wavelength 1.54 Å. The data were taken in the range of 5–70° (2θ) with a step size of 0.02°. The XRD line broadening measurements were carried out on a Rigaku D/MAX-rb diffractometer. The data were taken in the range of 23.5–27.0° (2θ) with a step size of 0.01°. The X-ray tube was operated at 40 kV and 120 mA. The divergence slit (DS) was 1.0°, the scattering slit (SS) was 1.0 mm and the reception slit (RS) was 0.15 mm.

The microphotographs of the TiO₂ powders and films were obtained using Jeol JEM 2010 high-resolution transmission electron microscope (HRTEM) equipped with a Link ISIS energy dispersive X-ray spectrometer (EDS) and Hitachi S-4500 scanning electron microscope (SEM).

Auger electron spectroscopy (AES) measurement of doped TiO₂ film was performed with a MicroLab 310-F instrument.

Simultaneous differential scanning calorimetric analysis (DSC) and thermogravimetric analysis (TG) were carried out in air on the TiO₂ gels on a 2960 SDT V3.0F instrument with a heating rate of 10 °C/min.

The specific surface area, pore volume and pore size distribution of TiO₂ powders calcined at 500 °C were obtained by N₂ adsorption/desorption method at –196 °C using a Micromeritics ASAP2010 automated apparatus. Powders were degassed at 100 °C prior to the

measurement. The specific surface area was determined by the multipoint Brunauer–Emmett–Teller (BET) method using the adsorption data in the relative pressure (P/P_0) range of 0.05–0.25. The pore size distribution data were calculated by the ASAP2010 software from the N₂ adsorption isotherms. The Barrett–Joyner–Halender (BJH) method with cylindrical pore size calculated from the Kelvin equation was used in the process.

3. Results

3.1. Influence of Ag doping on the TiO₂ phase transformation

Fig. 1 shows the XRD patterns of pure and doped TiO₂ powders calcined at different temperatures. Peaks marked “A” and “R” correspond to anatase and rutile phases, respectively. It can be seen that the anatase phase starts to appear while the TiO₂ powders are calcined at 400 °C. Calcined at 500 °C, both the pure and doped TiO₂ powders are well crystallized. For pure TiO₂ powder, the rutile phase does not appear until the powder is calcinated at about 750 °C. And a considerable amount of anatase remains in the powder while it is calcinated at 800 °C. For doped TiO₂ powders, however, the anatase to rutile transformation starts at lower temperatures. For the TiO₂ powder with 4 mol% Ag doped, the rutile phase appears while the powder is calcined at about 700 °C, and the phase transformation is completed at 800 °C. For the TiO₂ powder with 8 mol% Ag doped, the phase transformation occurs at about 650 °C, and all anatase transforms into rutile after a calcination at 700 °C. For the TiO₂ powder with 10 mol% Ag doped, the phase transformation even starts at about 600 °C and finishes at about 650 °C. This fact indicates that the Ag dopant promotes the anatase to rutile phase transformation, and it seems that the higher the Ag concentration, the lower the temperature at which the anatase to rutile transformation occurs.

The enhancement in the TiO₂ phase transformation can be attributed to the following three facts.

First, anatase grain sizes decrease in the presence of the Ag dopant and specific surface areas of TiO₂ powders with 2–6 mol% Ag doped increase. The rutile nucleation and grain growth in those TiO₂ powders is enhanced.

Using the Scherrer estimation: $D = K\lambda / (\beta_B - \beta_b) \cdot \cos\theta$, where D = average anatase grain sizes, K = Scherrer constant, λ = wavelength of radiation, β_B and β_b = the full width of the diffraction line at one half of the maximum intensity for the sample and the standard, respectively and θ corresponds to the peak position, the average anatase grain size of TiO₂ powders were determined from the broadening of the anatase (101) peak ($2\theta = 25.35^\circ$). The results are given in Table 1.

Compared with those of pure TiO₂ powders, for doped TiO₂ powders average anatase grain sizes decrease. Fig. 2 presents the HRTEM microphotographs of TiO₂ powders and Fig. 3 the SEM microphotographs. The microphotographs confirm that sizes of anatase grains decrease with the Ag doping. Especially for TiO₂ powders calcined at 500 °C, HRTEM microphotographs show that the anatase grain sizes decrease from ca. 20 nm for pure TiO₂ powder to ca. 10–15 nm for doped TiO₂ powders.

With the anatase grain size decreasing, the total boundary energy for TiO₂ powder increases. The driving force for rutile grain growth then increases and the anatase to rutile phase transformation is promoted.¹³

Table 1

Effects of calcination temperature and Ag concentration on the average anatase grain size (nm)

Ag concentration (mol%)	Calcinations temperature (°C)		
	500	600	700
Pure TiO ₂ powder	16	37	62
2	10	19	62
4	10	19	51
6	14	26	58
8	13	27	73*
10	14	30	155*

* Average rutile grain sizes, which are determined from the intensity of the rutile (110) peak ($2\theta = 27.45^\circ$).

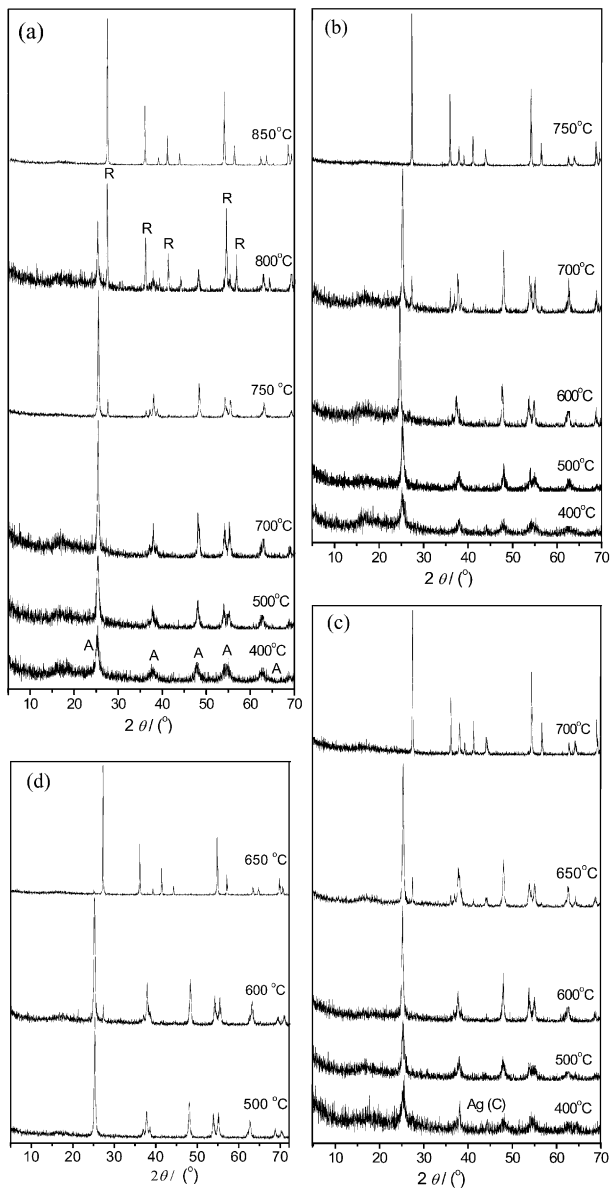


Fig. 1. XRD patterns of (a) pure TiO₂ powder and Ag-doped TiO₂ powders with (b) 4 mol%, (c) 8 mol% and (d) 10 mol% Ag doped.

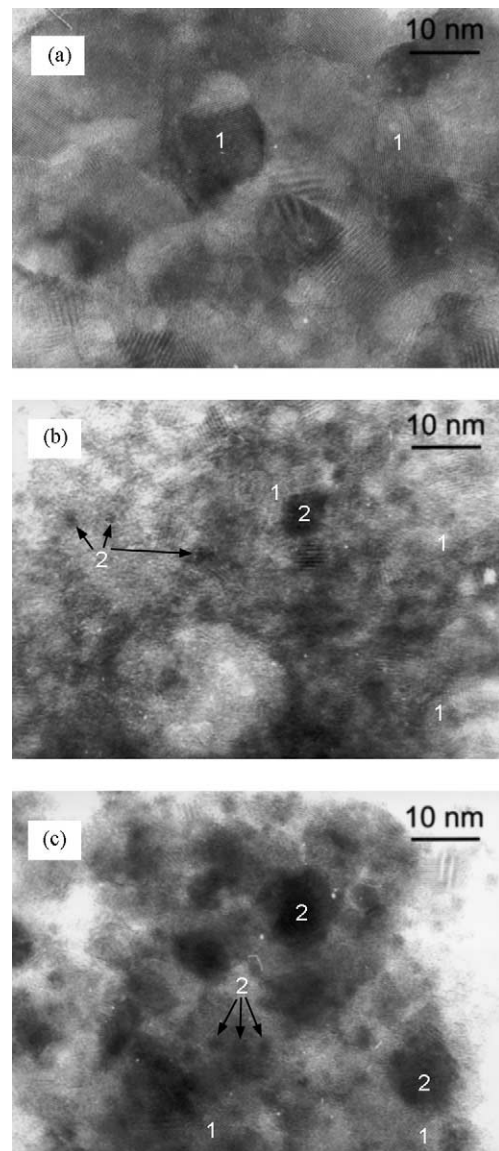


Fig. 2. HRTEM microphotographs of (a) pure TiO₂ powder, (b) 4 mol% and (c) 8 mol% Ag doped TiO₂ powders. The numerals 1 and 2 indicate TiO₂ grains and Ag particles, respectively, which were identified by the EDS analysis.

Besides, Table 2 presents the surface morphological characterization results for the pure and doped TiO_2 powders. It can be seen that corresponding to the anatase grain size decreasing, in a proper range, specific surface areas of doped TiO_2 powders increase, being 76, 63, and 58 m^2/g , respectively for TiO_2 powders with 2, 4 and 6 mol% Ag doped with respect to that of 45 m^2/g

for the pure TiO_2 powder. With the specific surface area increasing, the density of surface defects at the surface of anatase grains, which are considered the rutile nucleation sites for TiO_2 powders with relatively high specific surface areas,^{11,14} would increase. The rutile nucleation is then enhanced occurring at those surface defects and growing towards the bulk. The anatase to

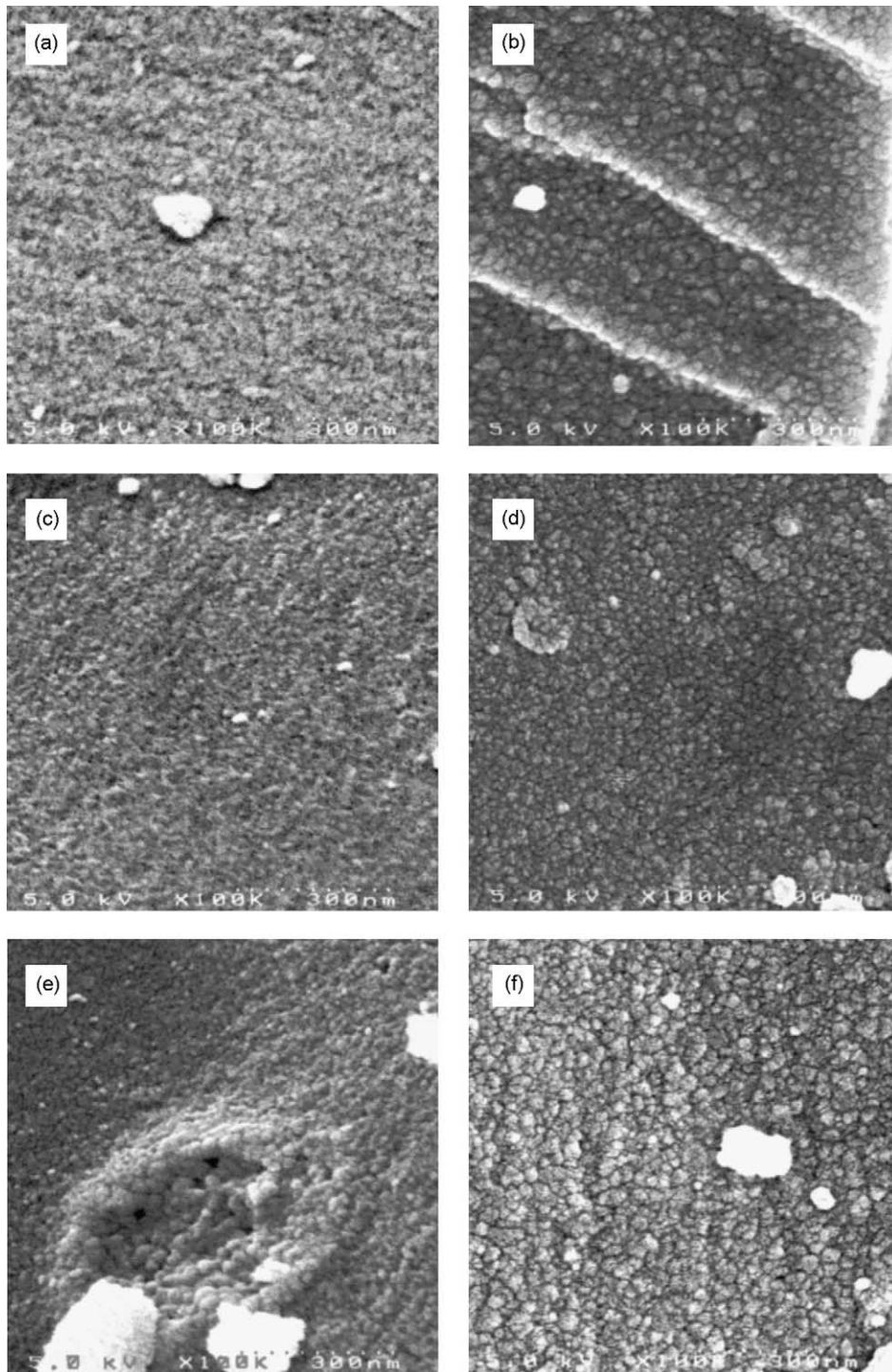


Fig. 3. SEM microphotography of pure TiO_2 powders calcined at (a) 500 °C and (b) 600 °C; 4 mol% Ag doped TiO_2 powders calcined at (c) 500 °C and (d) 600 °C; and 8 mol% Ag doped TiO_2 powders calcined at (e) 500 °C and (f) 600 °C, respectively.

rutile phase transformation in the powders is thereby promoted.

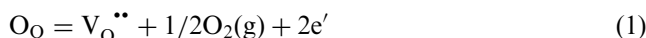
Secondly, with Ag doping, the concentration of oxygen vacancies at the surface of anatase grains increases, which favors the ionic rearrangement and structure reorganization for rutile phase.

It is well accepted that the concentration of oxygen vacancies strongly influences the rate of the anatase to rutile transformation.^{10,15} Because the radius of Ag⁺ ion (ca. 126 pm) is much larger than that of Ti⁴⁺ ion (ca. 68 pm), the Ag⁺ ions introduced by the sol-gel process could not enter into the lattice of anatase phase to form a stable solid solution. During the drying and calcination process with the elimination of liquids and organic substance and the crystallization of anatase phase, the uniformly dispersed Ag⁺ ions would gradually migrate from the volume of anatase grains to the surface and further to the surface of the TiO₂ powder under the action of heat. Fig. 4 shows the AES depth profile for 8 mol% Ag doped TiO₂ film coated three times on Si substrate. It's evident that the Ag dopants are accumulated in a layer with 30 nm in thickness and the concentration of Ag atoms at the film surface reaches 20 mol%, which gives the evidence that the major part of the Ag dopant eventually migrates to the surface of the TiO₂ support. Taking into account the investigation depth of the EDS analysis, ca. 20 nm in

this case, in Fig. 2b and c it can also be concluded that the Ag dopant is mainly distributed at the surface of the TiO₂ powders. The density of surfaces defects at the surface of anatase grains then increases, which favors the rutile nucleation.

On the other hand, due to the high redox potential for the Ag⁺ ion, by heat and TiO₂ photocatalytic reduction, the Ag⁺ ions spreading on the surface anatase grains would gradually be reduced into Ag⁰.^{16,17} Fig. 5 shows the XRD patterns for TiO₂ gel powders dried at 100 °C for 72 h. For doped TiO₂ gel powders we can see peaks corresponding to metallic silver, at 2θ = 38.1, 44.0 and 64.5°, respectively, indicating that the Ag⁺ ions are effectively reduced into Ag⁰ even while the TiO₂ gel is heat-treated at 100 °C for a long time [due to the low Ag content, however, such metallic Ag peaks could not be recognized in Fig. 1b and c. The strongest metallic Ag peak at 2θ = 38.1° may be overlapped by anatase (004) peak (2θ = 37.8°)].

For charge compensation, oxygen vacancies occur:



The concentration of oxygen vacancies at the surface of the TiO₂ powder then increases, which facilitates the bond rupture and ionic movement necessary for the formation of the rutile phase. The anatase to rutile phase transformation is then accelerated.

It is very interesting to note that for doped TiO₂ powders with Ag concentrations higher than 8 mol%, the phase transformation occurs at even lower temperatures though specific surface areas of the powders significantly decrease (see Table 2), for in those cases the two factors discussed above that accelerates the phase transformation in doped TiO₂ powders with Ag concentrations not exceeding 8 mol% can not explain such a strong enhancing effect. Although the concentration of anion vacancies at the surface of the powders may further increase with the Ag concentration, the phase

Table 2
Specific surface areas, average pore diameters and pore volumes for TiO₂ powders

Ag concentration (mol%)	BET specific surface area (m ² /g)	BJH average pore diameter (nm)	BJH pore volume (mm ³ /g)
Pure TiO ₂ powder	45	3	51
2	76	4	73
4	63	4	73
6	58	4	63
8	25	4	37
10	16	5	30

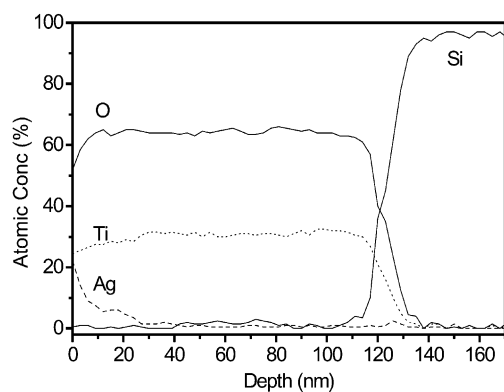


Fig. 4. AES depth profile of 8 mol% Ag doped TiO₂ film coated on the Si substrate and calcined at 500 °C.

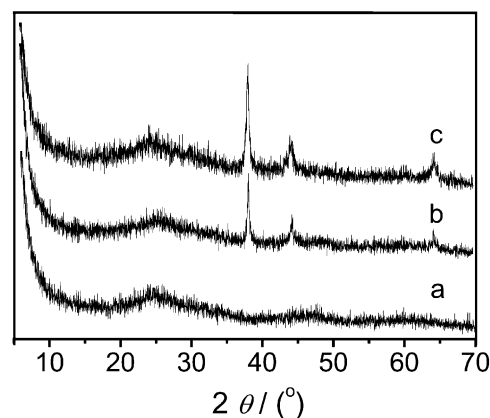


Fig. 5. XRD patterns of xerogel TiO₂ powders dried at 100 °C. (a) Pure TiO₂ powder, (b) 4 mol% and (c) 8 mol% Ag doped TiO₂ powders.

transformation would not be enhanced so strongly. That suggests that the Ag dopant probably promotes the phase transformation in those TiO₂ powders through other ways. Considering that the specific surface area of the TiO₂ powders markedly decrease, the phenomenon is probably caused by enhanced absorption of heat produced by the oxidation of organic groups and decomposition of nitrate contained in the TiO₂ gel powders during the calcination process.

Fig. 6 shows the DSC and TG traces for TiO₂ powders. It can be seen that in the DSC traces there are three exothermic peaks. According to the literature,^{18,19} the first two peaks in the temperature range of 200–

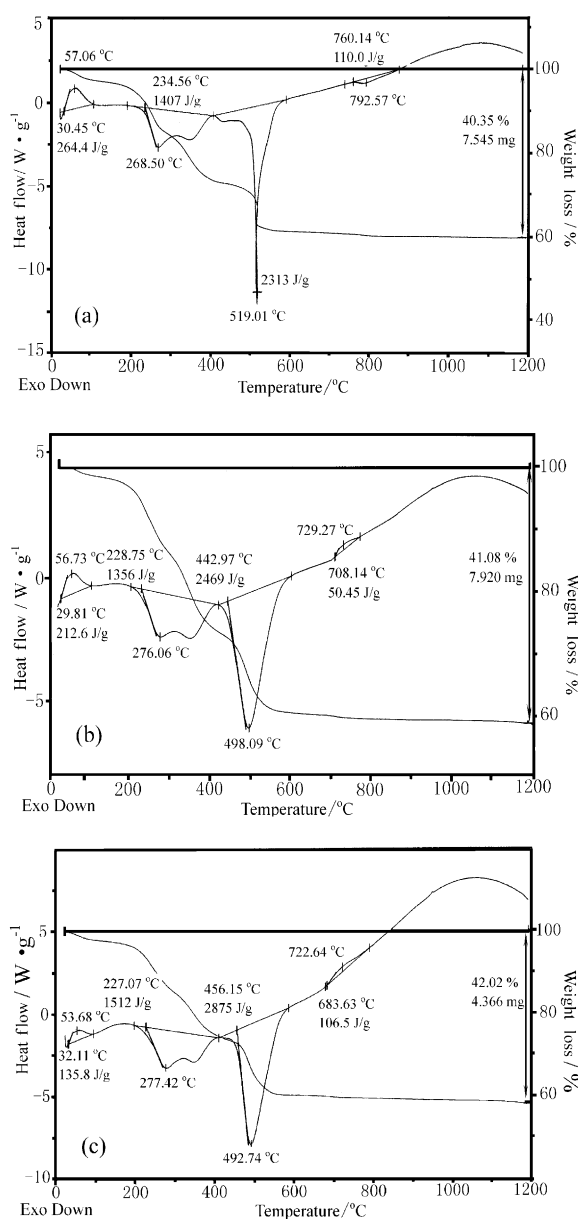


Fig. 6. DSC-TG curve of TiO₂ gel powders. (a) Pure TiO₂ powder, (b) 4 mol% and (c) 8 mol% Ag doped TiO₂ powders.

400 °C can be attributed to the oxidation of some organic substances and the TiO₂ amorphous to anatase phase transformation. Combined with the simultaneous 16–30% weight losses in the TG traces, the largest exothermal peaks in the temperature region of 400–600 °C can be attributed to the oxidation of organic groups contained in the TiO₂ gel powders and the decomposition of nitrate. The exothermal process in this temperature range evolves large amounts of heat (ca. 185–230 KJ/mol). According to the thermophysical data given by Lietz and Shomate,²⁰ the heat is completely sufficient to warm the anatase grains from about 500° to 750 °C, the anatase to rutile phase transformation point for the pure TiO₂ powder as determined by XRD. Temperatures higher than the transformation point would be obtained locally and the phase transformation would be greatly facilitated if the TiO₂ powder can effectively absorb the heat for the warming of anatase grains.

For the pure and doped TiO₂ powders with the Ag concentrations not exceeding 8 mol%, because the powders possess large specific surface areas, the large amount of heat produced by the oxidation of organic groups and decomposition of nitrate would escape rapidly and the TiO₂ powders could hardly effectively absorb it. For TiO₂ powders with 8 and 10 mol% Ag doped, however, specific surface areas of the powders markedly decrease to ca. 25 and 16 m²/g (the reason will be discussed in detail later). With the specific surface area decreasing, the total thermal conductivity of the powders would decrease.²⁰ The heat produced in the powders then cannot diffuse and escape so rapidly. Besides, in Fig. 6 it can be seen that for doped TiO₂ powders the exothermic peaks in the temperature range of 400–600 °C increase in intensity, being ca. 230 kJ/mol for the TiO₂ powder with 8 mol% Ag doped with respect to those of ca. 185 and 200 kJ/mol for the pure and 4 mol% Ag doped TiO₂ powders. Relatively the doped TiO₂ powders with Ag concentrations higher than 8 mol% then can absorb much more heat during this exothermic process for the warming of anatase grains. As a result the rutile nucleation would first start at defects in the bulk of the powders and grow towards the surface. And because the phase transformation itself is an exothermal phenomenon, the heat evolved would cause other new anatase grains to convert to rutile. The phase transformation in those TiO₂ powders is thereby promoted and occurs at much lower temperatures and higher speeds though the specific surface areas of the powders greatly decrease.

3.2. Influence of Ag doping on the anatase grain growth

Average anatase grain sizes decrease with the Ag doping, indicating that the Ag dopant has a depression effect on the anatase grain growth.

As discussed above, because of its relatively large radius, the Ag^+ ions introduced by sol-gel process could not enter into the lattice of TiO_2 phase. During the calcination process they would gradually migrate from the volume of anatase grains to the surface and further to the surface of TiO_2 powders. Those Ag^+ ions then would compete with Ti^{4+} and O^{2-} ions for the diffuse and reorganization, and the anatase crystallization and grain growth is impeded. Furthermore, because the Ag^+ ions gradually moves along with the anatase grain boundaries to the surface of TiO_2 powder, the energy necessary for the movement of anatase grain boundary would increase and the driving force for the anatase grain boundary migration consequently decreases.²²

Besides, the Ag^+ ions would strongly impede the rearrangement of Ti^{4+} and O^{2-} ions at the surface of anatase grains. As shown in Fig. 4, AES analysis shows that for the 8 mol% Ag doped TiO_2 film, the Ag concentration at the surface of the film reaches 20 mol%. For the TiO_2 powder with 4 mol% Ag doped, assuming the Ag concentration at the surface of the powder being 10 mol%, Ag^+ ions uniformly distributed at the surface of TiO_2 gel powder and at the early stage of the calcination process the specific surface area of the TiO_2 gel powder being twice as much as that of the eventual TiO_2 powder, the density of Ag^+ ions on the TiO_2 powder during the calcinations process can be estimated to be as high as 1 atom per 16.74 \AA^2 (for anatase, the lattice parameters are as follow: $a=3.784 \text{ \AA}$, $c=9.515 \text{ \AA}$).²¹ Those Ag^+ ions probably exist on TiO_2 powders by forming Ag–O–Ti bonds.¹⁷ The rearrangement of Ti^{4+} and O^{2-} ions at the surface of anatase grains then would be greatly disturbed. And the mutual contact and material transfer between anatase grains is hindered. Anatase grain growth is thereby depressed and anatase grain sizes decrease.

It should be noted that the decrease in the anatase grain size and increase in the density of active defects and concentration of oxygen vacancies at the surface of TiO_2 powders that promotes the anatase to rutile phase transformation have positive effects on the anatase grain growth. The Ag dopant has such a strong depression effect on the anatase grain growth that the anatase grain growth is after all depressed in the presence of Ag. It shows that the additive that speeds up the anatase to rutile phase transformation does not always have the enhancing effect on the anatase grain growth. It still depends upon the nature and content of the additive.

With the decrease in anatase grain sizes, in a proper range the specific surface areas of doped TiO_2 powders increase (see Table 2). For those TiO_2 powders during the photocatalysis more anatase grains would take part in the photoreaction and larger amounts of surface active sites would be present for the photocatalysis. It is favorable for the TiO_2 photocatalysis.

For the Ag^+ ions, as discussed above that under the action of heat and TiO_2 photocatalysis they would be gradually reduced into Ag^0 . Also because the Ag–O bonding is much weaker than Ti–O and Ag–Ag bonding and Ag atom possesses higher surface free energy than TiO_2 ,^{23–26} during the calcinations process the Ag atoms will have the tendency to aggregate into metallic Ag particles and clusters at about 2–10 nm, as shown in Fig. 2b (the Ag particles and clusters are identified by the EDS analysis).

Anatase grain sizes, however, would not further decrease with the Ag concentration. It can be seen in Fig. 2b and c that calcined at 500 °C, anatase grains in TiO_2 powders with 8 and 10 mol% Ag doped are bigger than those in the pure and other doped TiO_2 powders. And specific surface areas for TiO_2 powders with 8 and 10 mol% Ag doped correspondingly decrease. The reason needs to be further understood. But considering that the metallic Ag is easily to aggregate, the fact can be attributed to the early formation of metallic Ag particles and clusters during the calcination process with the increase in Ag^+ ion density. In that situation the depression effect of the Ag dopant on the growth of anatase grains is ended in a much shorter time and total depression effect of the Ag dopant on the anatase grain growth decreases. Contrarily with the increase in the density of surface defects and concentration of oxygen vacancies with increasing Ag concentration, calcination of anatase grains is enhanced. Anatase grain sizes then relatively increase and specific surface areas of the TiO_2 powders decreases.

Besides, for the TiO_2 powder with 8 mol% Ag doped, with the increase in the Ag dopant concentration, in Fig. 2c it can be seen that both the density and sizes of Ag particles and clusters increase. With the increase in the density of Ag particles and clusters, the blocking of pores at the surface of the TiO_2 powder by the Ag particles and clusters would increase. That leads to the decrease in the pore volume and surface area of the TiO_2 powder and also results in the decrease in the specific surface area of the TiO_2 powder. Specific surface areas of 8 and 10 mol% Ag doped TiO_2 powders therefore greatly decrease.

4. Conclusions

The anatase to rutile phase transformation and anatase grain growth in pure and Ag doped TiO_2 powders prepared by sol-gel method has been studied. It is found that the Ag dopant accelerates the TiO_2 anatase to rutile transformation. The mechanism, however, changes with the Ag concentration. It's also found that the Ag dopant has a depression effect on the anatase grain growth. Based on this, it is concluded that the additive that accelerates the anatase to rutile phase transformation

does not always promote the calcination of anatase grains. It depends upon the nature and loading of the additive.

At relatively low Ag concentrations (2–6 mol%), anatase grain sizes decrease and specific surface areas of TiO₂ powders increase. This makes the Ag doped sol-gel TiO₂ powder and film to be expected to possess higher photocatalytic activity.

Acknowledgements

Part of this work has been supported by the Chinese Ministry of Science and Technology and AFCRST (Association Franco-Chinoise pour la Recherche Scientifique et Technique).

References

- Hoffman, M. R., Martin, S. T., Choi, W. and Bahnemann, D. W., Environmental application of semiconductor photocatalysis. *Chem. Rev.*, 1995, **95**, 69–96.
- Fujishima, A., Rao, T. N. and Tryk, D. A., Titanium dioxide photocatalysis. *J. Photochem. Photobiol. C: Photochem. Rev.*, 2000, **1**, 1–21.
- Herrmann, J. M., Heterogeneous photocatalysis: fundamental and applications to the removal of various types of aqueous pollutants. *Catal. Today*, 1999, **53**, 115–129.
- Teeng, I. H., Chang, W. C. and Wu, J. C. S., Photoreduction of CO using sol-gel derived titania and titania-supported copper catalysts. *Appl. Catal. B: Environm*, 2002, **37**, 37–48.
- Navio, J. A., Testa, J. J., Djedjeian, P., Padron, J. R., Rodriguez, D. and Litter, M. I., Iron-doped titania semiconductor powders prepared by a sol-gel method. Part I: synthesis and characterization. *Appl. Catal. A: General*, 1999, **177**, 111–120.
- Yuan, Z. H., Jia, J. H. and Zhang, L., D, Influence of co-doping of Zn (II)+Fe (III) on the photocatalytic activity of TiO₂ for phenol degradation. *Mater. Chem. Phys*, 2002, **73**, 323–326.
- Lopez, T., Gomez, R., Pecci, G., Reyes, P., Bokhimi, X. and Novaro, O., Effect of pH on the incorporation of platinum into the lattice of sol-gel titania phases. *Mater. Lett.*, 1999, **40**, 59–65.
- Yamashita, H., Harada, M., Misaka, J., Takeuchi, M., Ikeue, K. and Anpo, M., Degradation of propanol diluted in water under visible light irradiation using metal ion-implanted titanium dioxide photocatalysts. *J. Photochem. Photobiol*, 2002, **148**, 257–261.
- Iida, Y. and Ozaki, S., Grain growth and phase transformation of titanium oxide during calcination. *J. Am. Ceram. Soc.*, 1961, **44**(3), 120–127.
- MacKenzie, K. J. D., The calcinations of titania, part V: kinetics and mechanism of the anatase/rutile transformation in the presence of additives. *Trans. J. Brit. Ceram. Soc.*, 1975, **74**, 77–84.
- Amores, J. M. G., Escribano, V. S. and Busca, G., Anatase crystal growth and phase transformation to rutile in high-area TiO₂, MoO–TiO₂ and other TiO₂ supported oxide catalytic systems. *J. Mater. Chem.*, 1995, **5**(8), 1245–1249.
- He, C., Yu, Y., Hu, X. F. and Larbot, A., Influence of Ag doping on the structure and photocatalytic activity of TiO₂. *Appl. Surf. Sci.* (in press).
- Oliveri, G., Ramis, G., Busca, G. and Escribano, V. S., Thermal stability of vanadia-titania catalysis. *J. Mater. Chem.*, 1993, **3**(12), 1239–1249.
- Amores, J. M. G., Escribano, V. S., Busca, G. and Lorenzelli, V., Solid-state and surface chemistry of CuO–TiO₂ (Anatase) powders. *J. Mater. Chem.*, 1994, **4**(6), 965–971.
- Hishita, S., Mutoh, I., Koumoto, K. and Yanagida, H., Inhibition mechanism of the anatase-rutile phase transformation by rare earth oxides. *Ceram. Intern*, 1982, **9**(2), 61–67.
- Litter, M. I., Heterogeneous photocatalysis: transition metal ions in photocatalytic systems. *Appl. Catal. B: Environ*, 1999, **23**, 89–114.
- Epifani, M., Giannini, C., Tapfer, L. and Vasanelli, L., Sol-gel synthesis and characterization of Ag and Au nanoparticles in SiO₂, TiO₂ and ZrO₂ thin films. *J. Am. Ceram. Soc.*, 2000, **85**(10), 2385–2393.
- Navio, J. A., Macias, M., Gonzalez-Catalan, M. and Justo, A., Bulk and surface characterization of powder iron-doped titania photocatalysts. *J. Mater. Sci.*, 1992, **27**, 3036–3042.
- Xu, Q. and Anderson, M. A., Sol-gel route to synthesis microporous ceramic membranes: thermal stability of TiO₂-ZrO₂ mixed oxides. *J. Am. Ceram. Soc.*, 1993, **76**(8), 2093–2097.
- Goldsmith, A., Waterman, T. E. and Hirschhorn, H. J., *Handbook of Thermophysical Properties of Solid Materials*, Vol. III—Ceramics. Pergamon Press Ltd., London, 1961, pp. 237–240.
- Howard, C. J., Sabine, T. M. and Dickson, F., Structural and thermal parameters for rutile and anatase. *Acta Crystallogr. B*, 1991, **47**, 462–468.
- Kingery, W. D., Bowen, H. K. and Uhlmann, D. R., *Introduction to Ceramics*, 2nd ed. John Wiley and Sons, New York, 1976, pp. 448–459.
- Chen, D. A., Bartelt, M. C., Seutter, S. M. and McCarty, K. F., Small, uniform and thermally stable silver particles on TiO₂ (110)-(1x1). *Surf. Sci.*, 2000, **464**, L708–L714.
- Bates, S. P., Kresse, G. and Gillan, M. J., A systematic study of the surface energetics and structure of TiO₂ (110) by first-principles calculations. *Surf. Sci.*, 1997, **385**, 386–394.
- Vitos, L., Buban, A. V., Skriver, H. L. and Kollar, J., The surface energy of metals. *Surf. Sci.*, 1998, **411**, 186–202.
- Wu, J. M. and Chen, C.-J., Dielectric properties of (Ba, Nb) doped TiO₂ ceramics: migration mechanism and roles of (Ba, Nb). *J. Mater. Sci.*, 1988, **23**, 4157–4164.